Hall Effect In Indium Antimonide
Third Year Lab Report

James Parker: 10694426
Department of Physics and Astronomy, University of Manchester
(Experiment performed in collaboration with R. Soares)
(Dated: December 15, 2023)

This experiment investigated the Hall Effect in a sample of impure Indium Antimonide across temperatures varying from 77k to 400k. The results indicated a band gap of $0.226 \pm 0.001eV$ in agreement with the expected value. The sample showed p-type behaviour at low temperatures. Within the intrinsic region, carrier concentration and mobility followed expected relationships with temperature. A positive linear magnetoresistance was found, indicating an absence of quantum mechanical influences on resistance.

1. INTRODUCTION

The Hall Effect, discovered by Edwin Hall, occurs when a magnetic field is applied perpendicular to an electric current in a conductor, resulting in a Hall voltage across the material [1]. This effect provides insights into the nature and behaviour of charge carriers in a material.

Semiconductors have a unique band structure allowing thermal excitation of electrons from the valence to conduction bands at practical temperatures. They exhibit varying conductivity based on temperature and doping levels. In semiconductors, the Hall Effect is more pronounced due to higher charge carrier mobility. Indium Antimonide (InSb), with its small band gap and high electron mobility [2], is an ideal candidate for Hall Effect experiments, especially for observing temperature effects on carrier concentration around room temperature.

This experiment aims to measure the resistance and Hall coefficient of an impure InSb crystal across temperatures ranging from 77K to 400K. These measurements will help deduce the sample's band gap, carrier concentration, impurity concentration, mobility, and doping type.

2. THEORY

Semiconductors like InSb have different conduction behaviours in different temperature regions due to the energy gap between the valence and conduction bands. There are two key regions: the extrinsic region where conductivity is primarily due to dopant atoms with a low ionisation energy, and the intrinsic region where conductivity is primarily due to intrinsic charge carriers created by thermal generation of electron-hole pairs [3].

2.1. Resistance

To find values for resistance at different temperatures, we want to obtain a linear relationship between voltage and current in the sample due to non-linear response that is possible at high current from Joule heating and carrier saturation [4].

In the intrinsic region, conductivity is given by

$$\sigma_i = n_i \mu_e e + p_i \mu_h e, \tag{1}$$

where e is the charge of an electron, μ_e and μ_h are the mobilities of electrons and holes, respectively, p_i and n_i are the intrinsic concentration of holes and electrons respectively, which are approximately equal in the intrinsic region. The intrinsic carrier concentration is given by

$$n_i = \sqrt{N_c N_v} \cdot e^{-\frac{E_g}{2kT}}, \tag{2}$$

where N_c and N_v are the effective density of states in the conduction and valence bands respectively, and E_g is the energy band gap. N_c and N_v both have a dependence on T as $N_{v/c} \propto T^{3/2}$. Since resistance is proportional to the inverse of conductivity,

$$R \propto T^{-3/2} e^{\frac{E_g}{2kT}}. \tag{3}$$

2.2. Band Gap

The band gap of the sample at 0k can be found from Equation 3, approximating it to just the exponential term. At high temperatures, $e^{\frac{-E_g}{2kT}}$ becomes the dominant factor because E_g is much larger than the product kT. Plotting a graph of $ln(R)\ vs\ \frac{1}{T}$, we can extract a value for the band gap from the gradient.

2.3. Hall coefficient

The Hall coefficient represents the ratio of the induced electric field to the product of the current density and the applied magnetic field in a material. The Hall coefficient's value and sign provide insights into the carrier concentration and mobility. The Hall coefficient is defined as

$$R_H = \frac{V_H \cdot t}{I \cdot B}, \tag{4}$$

where V_H is Hall voltage, t is the thickness of the sample, and I and B represent the sample current and magnetic field strength respectively. By plotting $V_H\ vs\ I \cdot B$, we can find the Hall coefficient for individual temperature values.

2.4. Sample Type

In the intrinsic region, there are approximately an equal number of electrons and holes. Electrons usually have a higher mobility than holes as they are less impeded by the lattice structure of the semiconductor, so contribute more to Hall voltage [5]. In the intrinsic region the Hall voltage observed will be due to electrons.

To determine sample type, we will inspect the extrinsic region where the dominant charge carriers are from dopants. The sign of the Hall coefficient can be used along with the sign of the Hall voltage to determine the sample type.

2.5. Carrier Concentration

We can determine carrier concentration from the Hall coefficient using,

$$R_H = \frac{1}{ne}, \tag{5}$$

where n is the carrier concentration. Using Equation 3 with the same approximation used in Section 2.2, we expect an exponential increase in carrier concentration with temperature in the intrinsic region.

2.6. Mobility

Mobility of charge carriers is given by

$$\mu = \rho \cdot R_H \tag{6}$$

where μ is mobility and ρ is resistivity. The mobility of charge carriers follows a negative power law relationship with temperature [5],

$$\mu \propto T^{-m} \tag{7}$$

where m is a constant depending on the dominant scatter mechanism. This behaviour is a consequence of the increased lattice vibrations at higher temperatures, which lead to more frequent scattering of charge carriers, thereby reducing their mobility.

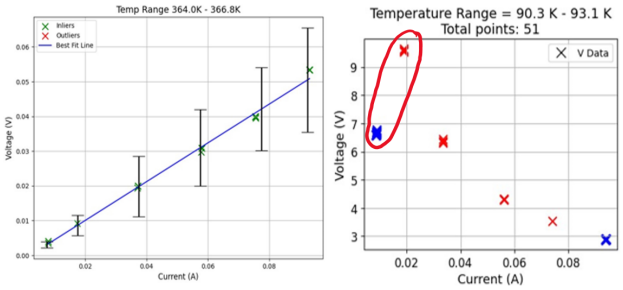

FIG. 1. Plots of Sample Voltage vs Sample Current. Left: example plot from intrinsic region. Right: example plot from extrinsic region with ohmic region circled in red.

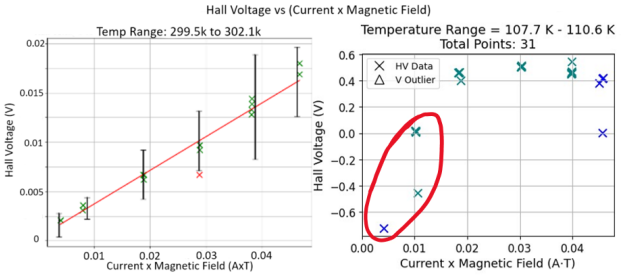

FIG. 2. Plots of $V_H vs (I \cdot B)$. Left: example plot from intrinsic region. Right: example plot from extrinsic region with ohmic region circled in red.

3. EXPERIMENTAL APPROACH

3.1. Experiment setup

The InSb sample was mounted on a cold finger within a vacuum, positioned in a homogeneous magnetic field. The cold finger facilitated cooling of the sample by conducting cryogenic temperatures from a liquid nitrogen reservoir. Temperature regulation was achieved through a heating element which operated in the variance between an adjustable set voltage and a temperature-correlated measured voltage. Measurement of sample voltage, current, Hall voltage and thermocouples voltage was conducted by a digital voltmeter, while a Hall probe measured magnetic field strength. Data recording for each parameter was automated at 16-second intervals.

3.2. Method

Direct measurements of sample voltage, current, temperature, Hall voltage, and magnetic field strength were conducted. The objective was to determine sample voltage and Hall voltage for given current values across a temperature spectrum from 77K to 400K, under a sufficiently strong magnetic field to elicit a significant Hall voltage.

The initial method involved maintaining a constant magnetic field of 0.5 Tesla, and varying the sample current at fixed temperatures, using increments of 0, 20, 40, 60, and 80 mA. For magnetoresistance analysis, this approach was replicated across magnetic field strengths of 0, 0.175, 0.35, 0.525, and 0.7 Tesla.

Sample temperature stability presented challenges, particularly at lower temperatures, due to a 16-second delay in temperature feedback and the need to balance cooling and heating influences. Efforts were made to maintain the temperature within a $\pm 1.5k$ range for each set temperature.

Subsequently, our strategy was updated to obtain results for a continuous temperature range. This involved fixing the magnetic field at 0.5 Tesla and the current, while allowing the sample temperature to gradually vary, thereby spanning the entire temperature range, repeating for the current values stated.

4. RESULTS

4.1. Resistance

In the extrinsic region, Ohm's law was applicable for currents ranging from 0 to approximately 20mA, indicated in Figure 1 (right), which is a shorter range than the intrinsic region, where Ohmic behaviour was observed across the entire examined current range of 0 to 100mA, illustrated in Figure 1 (left). This behaviour can be attributed to the effects of Joule heating and charge carrier saturation. A more comprehensive data set within the 0 to 20mA range could potentially provide enhanced insights into resistance characteristics in this region.

4.2. Hall Coefficient

In the intrinsic region, as detailed in Section 2.4, electrons govern the Hall effect. Our observations in this region revealed a positive Hall voltage sign. Therefore, a positive reading corresponds to electron dominance while a negative reading indicates hole dominance.

The validity of our Hall coefficient measurements is constrained to the current ranges where Ohm's law is applicable. In the extrinsic region, the limited data points within this ohmic region restrict our observations, resulting in small evidence of linearity at lower currents, as shown in Figure 2 (right).

In the intrinsic region, we obtain a linear relationship for the entire current and magnetic field range we measured, shown in Figure 2 left.

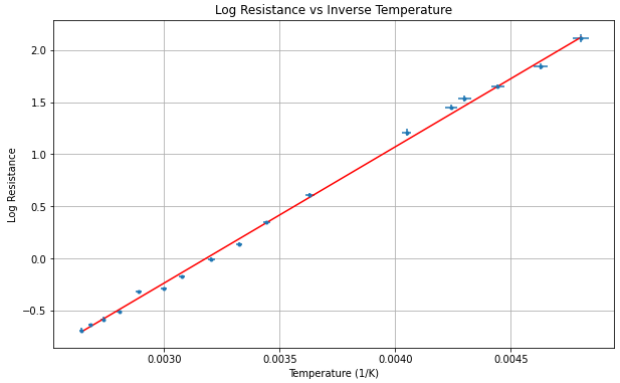

FIG. 3. Plot of $ln(R) vs \frac{1}{T}$ for the intrinsic region of the sample of impure InSb.

4.3. Band Gap

From Figure 3, the band gap of the InSb sample at $0k$ was found to be $0.226 \pm 0.001eV$. This is in favourable agreement with the expected value of $0.235eV$ [2].

4.4. Sample type

In the extrinsic region, our data is constrained by the limited Ohmic range, impacting the precision of our Hall coefficient analysis at these temperatures. Nonetheless, within this ohmic region, a negative Hall voltage was recorded, suggesting that holes are the predominant charge carriers, indicative of p-type doping in the sample. If the sample was n-type doped, we would not expect a sign inversion in Hall voltage, as electrons would be the dominant charge carrier at all temperatures. The absence of a negative Hall voltage reading in the intrinsic region further implies that the observed behaviour is intrinsic to the sample and not due to a measurement error.

4.5. Carrier concentration and impurity concentration

We see in Figure 4 that intrinsic carrier concentration increases exponentially with temperature.

To estimate the impurity concentration, we apply Equation 5 within the extrinsic region, assuming that $n_{total} \approx n_{dopant}$. This yielded an impurity concentration of $1.1 \times 10^{20} \pm 2 \times 10^{17}$ m^{-3}, which equates to roughly 10^{10} dopant atoms per cubic meter. However, this estimate is subject to

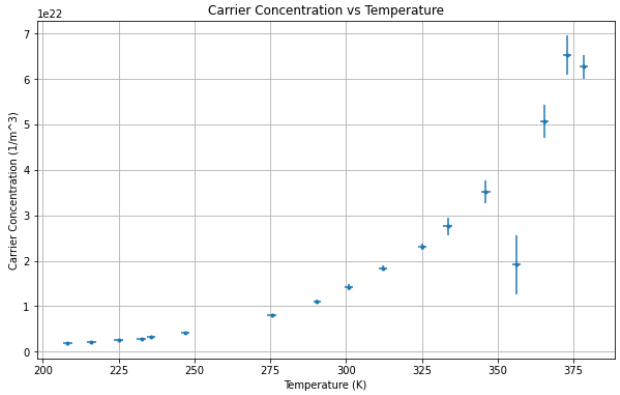

FIG. 4. Plot of Carrier Concentration *vs* Temperature.

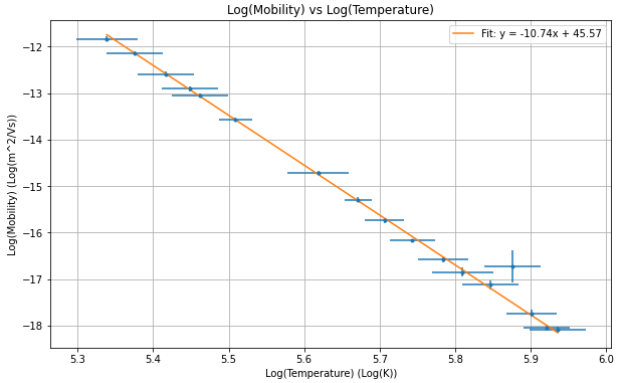

FIG. 5. Plot of $log(\mu)\, vs\, log(T)$

a degree of uncertainty, as it is derived from Hall coefficient values calculated from a limited subset of data that adheres to Ohm's law within the extrinsic region.

4.6. Mobilities

We observe a negative power relationship between carrier mobility and temperature within the intrinsic region as expected, showcased in Figure 5, with a measured *m* of 10.74 ± 0.46, shown in Figure 5.

4.7. Magnetoresistance

A positive magnetoresistance was observed in the sample. A linear relationship was found, which can be attributed to the Lorentz force increasing the path length for charge carriers which increases resistance. Linearity also indicates an absence of significant quantum mechanical influences such as quantum tunnelling or quantum Hall effects, which typically create non-linear resistance behaviours under magnetic fields [6]. An example is shown for 290k in Figure 6.

4.8. Source of Errors

Temperature was the primary source of errors, from random fluctuations due to thermocouple errors and human errors when attempting to maintain the temperature of the sample. Considering the significant impact of temperature fluctuations on the experiment's outcomes, it is more practical to focus on temperature errors, as they will have a greater effect on the results than the relatively minor resolution errors from measurements.

For a given current, we plotted sample voltage and Hall voltage against temperature respectively. A line of best fit for each plot was determined, and around this line of best fit a band corresponding to a one-standard-deviation range was established. This enabled a determination of a corresponding sample or Hall voltage range for a given temperature interval.

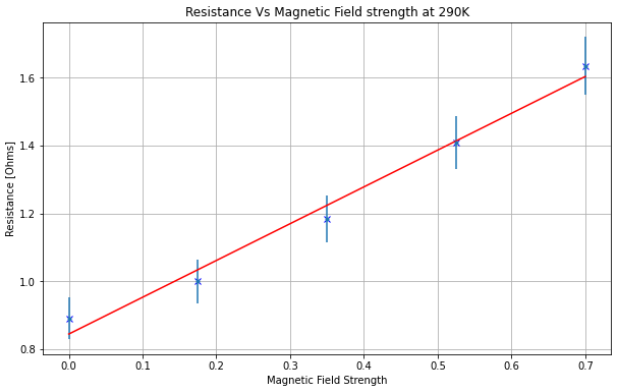

FIG. 6. Plot of Resistance *vs* Magnetic Field Strength at 290k.

5. CONCLUSIONS

The experiment quantified the band gap of the InSb sample as $0.226 \pm 0.001eV$, a finding that is consistent with established characteristics of InSb.

At lower temperatures, the sample demonstrated p-type behavior, a conclusion supported by the Hall voltage readings within the ohmic region, signifying holes as the majority carriers. An impurity concentration of $1.1 \cdot 10^{20} \pm 2 \cdot 10^{17} m^{-3}$ was found, which is indicative of a relatively high level of doping .

A notable observation was the exponential increase in carrier concentration with temperature, a hallmark of semiconductor behaviour in the intrinsic region. This was accompanied by a mobility of charge carriers that displayed an inverse power-law relationship with temperature, aligning with theoretical predictions.

The experiment also revealed a positive linear magnetoresistance in the sample, suggesting that the Lorentz force's effect on the path length of charge carriers predominantly contributes to the increased resistance under magnetic fields, rather than quantum mechanical influences.

Challenges encountered in maintaining stable temperature conditions were mitigated through error analysis methods, allowing for a more accurate integration of these uncertainties into our results.

For future improvement, employing smaller current increments at lower temperatures could provide more detailed insights in the ohmic region, prior to the onset of Joule heating and significant changes in carrier concentration. This approach could enhance the precision and depth of the analysis in these critical temperature ranges.

[1] E. H. Hall, American Journal of Mathematics **2**, 287 (1879).
[2] D. S. C.L. Littler, Applied Physics Letters **46**, 986 (1985).
[3] N. Balkan and A. Erol, *Semiconductors for Optoelectronics: Basics and Applications* (Springer Nature Switzerland AG, 2021) pp. 59–70.
[4] N. Balkan and A. Erol, *Semiconductors for Optoelectronics: Basics and Applications* (Springer Nature Switzerland AG, 2021) pp. 73–76.
[5] N. Balkan and A. Erol, *Semiconductors for Optoelectronics: Basics and Applications* (Springer Nature Switzerland AG, 2021) pp. 81–87.
[6] J. S. Hu and T. F. Rosenbaum, Nature Materials **7**, 10.1038/nmat2259 (2008).